

---

# The Complete Star Formation History of the Universe

Alan Heavens<sup>1</sup>, Benjamin Panter<sup>1</sup>, Raul Jimenez<sup>2</sup>, James Dunlop<sup>1</sup>

<sup>1</sup>Institute for Astronomy, University of Edinburgh, Blackford Hill, Edinburgh EH9-3HJ, UK; afh, bdp, jsd@roe.ac.uk

<sup>2</sup>Department of Physics & Astronomy, University of Pennsylvania, 209 South 33rd Street, Philadelphia, PA 19104-6396, USA; raulj@physics.upenn.edu

---

The determination of the star-formation history of the Universe is a key goal of modern cosmology, as it is crucial to our understanding of how structure in the Universe forms and evolves. A picture has built up over recent years, piece-by-piece, by observing young stars in distant galaxies at different times in the past[1]-[12]. These studies indicated that the stellar birthrate peaked some 8 billion years ago, and then declined by a factor of around ten to its present value. Here we report on a new study which obtains the complete star formation history by analysing the fossil record of the stellar populations of 96545 nearby galaxies. Broadly, our results support those derived from high-redshift galaxies elsewhere in the Universe. We find, however, that the peak of star formation was more recent - around 5 billion years ago. Our study also shows that the bigger the stellar mass of the galaxy, the earlier the stars were formed. This striking result indicates a very different formation history for high- and low-mass formation.

The optical stellar spectrum of a galaxy can be used as a probe of both its past star formation history, and the metallicity of its gas as a function of time. The spectra of a large sample of nearby galaxies therefore acts as a useful fossil record of the star formation rate (SFR) of the Universe, allowing estimates of the SFR over a very wide range of cosmic time, from the same internally consistent data set, and with very small statistical errors. The alternative is to use the finite speed of light to view galaxies at different cosmic epochs, and to look for signs of recent star formation. The present method decouples the star formation from the mass assembly - it takes into account all stars which end up in normal galaxies today, and it is much less sensitive to the large corrections, for extinction and for unobserved small galaxies, which must be applied to high-redshift studies.

The spectral data used in this analysis come from the Sloan Digital Sky Survey data release 1 (SDSS DR1), from an area of 1360 square degrees. The main sample has red apparent magnitude limits of  $15.0 \leq m_R \leq 17.77$ , and we also place a cut on surface brightness of  $\mu_R < 23.0$  (see [13] for discussion of this). The redshift range is  $0.005 < z < 0.34$ , with a median of 0.1. This leaves 96545 galaxies in this study. Full details of the

SDSS are available at <http://www.sdss.org/>. The spectra are top-hat smoothed to  $20\text{\AA}$  resolution, for comparison with the models of Jimenez et al[14], and emission-line regions are removed, as these are generally non-stellar and outside the scope of the theoretical model employed.

The speed of MOPED means we are not restricted to assuming simple parametrizations of the star formation history[15, 16]. For each spectrum, we recover the mass of stars created in 11 time periods, which are mostly equally spaced logarithmically in look-back time, separated by factors of 2.07, but with the first boundary at a redshift of 2. We assume a Salpeter initial mass function, and a cosmology given by the best-fitting parameters determined by the WMAP satellite[17]:  $\Omega_m = 0.27$ ,  $\Omega_v = 0.73$ ,  $H_0 = 71 \text{ km s}^{-1} \text{ Mpc}^{-1}$ . For each time period, we also recover the average metallicity of the gas, and an overall dust parameter for the galaxy, assuming a Large Magellanic Cloud extinction curve[18]. Thus we have a 23-dimensional parameter space to search. A straightforward maximum likelihood solution using the full spectrum of all the SDSS galaxies is impractical, so we use the patented radical lossless data compression algorithm MOPED [19] to compress each spectrum to 23 numbers, and we find the set of 23 parameters which fit these MOPED coefficients most accurately. The massive data compression allows much faster determination of the parameters and the errors on them, and, importantly, can be shown to be lossless in ideal cases, in the sense that the error bars are not increased by using the MOPED coefficients rather than the entire spectrum. More details are given in papers developing and testing MOPED[19, 20, 21].

With this method, we obtain the mass of stars created in each galaxy  $g$  in each period of time (relative to the time of emission of the galaxy light),  $\delta M_{*g}(t)$ . After redistribution of the stars to a set of time bins fixed in cosmic time, we estimate the star formation rate per unit co-moving volume by  $\dot{\rho}_*(t) = \sum_g \delta M_{*g} / (V_{\text{max}} \delta t)$ , where  $\delta t$  is the width of the time bin.  $V_{\text{max}}$  is the maximum volume in which the galaxy could be placed and still contribute to the star formation rate estimate at time  $t$ . Since we have no knowledge of the star formation rate at redshifts less than the observed redshift of the galaxy, this introduces a redshift cutoff. Other limits come from the magnitude and surface brightness limits of the sample. These are calculated by computing the galaxy spectrum as a function of time (from the recovered SFR parameters) and computing the expected observed  $R$ -band flux and surface brightness. We take account of the 3 arc sec fibre aperture by correcting the spectrum upwards by the ratio of the flux in  $R$  in a Petrosian radius (determined by the photometry) to the fibre flux. For individual galaxies this is likely to fail, but for the population as a whole there is evidence from the colours [16] that fibre-placing is such that there is no significant systematic difference in the sampling of stellar populations by the spectroscopy and photometry.

In Fig. 1 we show the co-moving star formation rate determined by MOPED and SDSS DR1, as a function of redshift, along with results from other determinations, largely based on instantaneous star formation rate indicators (UV flux,  $\text{H}\alpha$  emission, sub-mm emission etc). At a basic level the new data show good agreement over the redshift range of  $0.01 < z < 6$ . The low-redshift decline of SFR is clearly seen, and the SFR appears

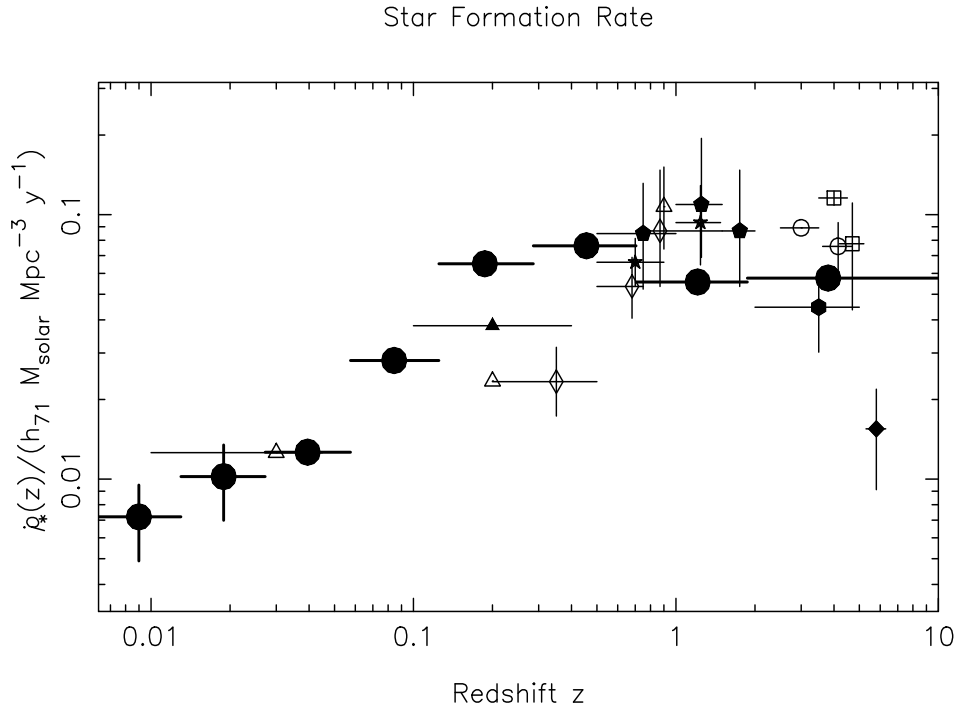


Figure 1: The star formation history of the Universe. The star formation rate recovered from the “fossil record” in the SDSS is shown by the eight large filled circles. The horizontal error bars represent the size of the bin in redshift. Vertical errors are bootstrap errors, and are invisibly small for most bins. The other symbols correspond to independent determinations using instantaneous measurements of the star formation rate, as follows;  $H\alpha$  measurements are open triangles at  $z \simeq 0.03$ [1],  $z \simeq 0.2$ [5],  $z \simeq 0.9$ [6]; UV from Subaru[11] (open squares), GOODS[12] (filled diamond), HST etc[3] (open circles), CFRS[2] (open diamonds), HDF[4] (filled pentagons), galaxies[7] (stars), galaxies[8] (filled triangle). The filled hexagon at  $z = 3.5$  represents a new estimate of the star-formation density provided by sub-mm galaxies in the redshift range  $2 < z < 5$ . This was derived by integrating the sub-mm source number counts[9] down to  $S_{850\mu\text{m}} = 1$  mJy, and assuming that 75% of such sources lie at  $z > 2$  (in line with recent redshift measurements[10]). In general the agreement is very good. However, there are two important results in our study which result from the extremely small vertical error bars. First, we find that 26% of the mass of stars in the present-day Universe were formed at  $z > 2$ . Second, while we confirm the previous measurements of a generally high level of star-formation activity at  $z \simeq 1$ , we find that global star-formation density peaked at significantly lower redshifts than previously claimed, in the bin spanning the redshift range  $0.3 < z < 0.8$ . The reason for this difference is clarified in Figure 2.  $h_{71}$  is the Hubble constant in units of  $71 \text{ km s}^{-1} \text{ Mpc}^{-1}$ .

to have flattened. Moreover, the level of star-formation activity inferred at high-redshift ( $z > 2$ ) is in rather good agreement with the completely independent values inferred from observations of high-redshift galaxies, suggesting that the dust corrections made in such studies are reasonable, if a little overestimated. The broad agreement of the SFR determined locally from the fossil record of the SDSS with the determinations from high-redshift galaxies gives support for the Copernican Principle, i.e. that the Earth has no special location in the Universe. It also supports the current standard cosmological model, as the volume elements assumed in the high-redshift studies are sensitive to the cosmological parameters. Note, however, that this does assume that our assumption about the initial mass function is reasonable, as we are inferring the number of early-forming high-mass stars (now dead) from the numbers of early-forming low-mass stars, which are still contributing to the galaxy spectrum.

One of our main results is that the period of star formation is broader than previously thought, and occurs at a lower redshift  $z \simeq 0.6$ , rather than 1 or more. Specifically, we find that 26% of the mass of stars in the present-day universe was formed at  $z > 2$  (cf [22]). The average metallicity rises from 0.44 (relative to Solar) at high  $z$  to a peak of 0.8 at  $z \simeq 1$  before declining to a level around 0.25 at the present time.

As we explain below, we believe our result differs because it includes the contributions made by all galaxies over a very wide mass range, extending down to galaxies with  $L \sim 2 \times 10^{-3} L_*$ . Note that virtually all 96545 galaxies contribute to the  $z > 0.3$  bins, so the statistical errors (bootstrap estimates) are negligible in comparison with modelling uncertainties and residual uncertainties in flux calibration. We also note that because we are not dominated by statistical errors, the errors are smaller in this approach than by analysing, for example, some appropriately-weighted average of the spectra themselves. Supplementary Information Figure 1 shows that parameter recovery is robust.

Our second major result is apparent when we present the star formation history of the sample divided into different ranges of observed stellar mass. We see strikingly in Fig. 2 that the redshift at which star-formation activity peaks is an essentially monotonically increasing function of final stellar mass. Star-formation activity in the galaxies in the lowest mass bins ( $M_* \simeq 10^{10} M_\odot$ ) peaked at  $z \simeq 0.2$ , while for galaxies an order of magnitude more massive the peak lies at  $z \simeq 0.5$ . At still higher masses, galaxies with masses comparable to a present-day  $L_*$  galaxy appear to have experienced a peak in activity at  $z \simeq 0.8$ , while the highest-mass systems ( $M_* > 10^{12} M_\odot$ ) show a monotonic decline in SFR in our data, with any peak constrained to lie at  $z > 2$ . This provides a natural explanation for why the most massive star-forming systems, such as the luminous sub-mm selected galaxies, should be largely found to lie at high-redshift ( $z > 2$ ; [10]) while at the same time providing further evidence that the bright sub-mm galaxies are indeed the progenitors of today's massive ellipticals [23]. The importance of low-mass systems in low-redshift star formation has been noted for example by [24] and [25].

Indeed, the strong mass-dependence of the star formation history provides a natural explanation of the high redshift of peak star formation activity seen in other surveys,

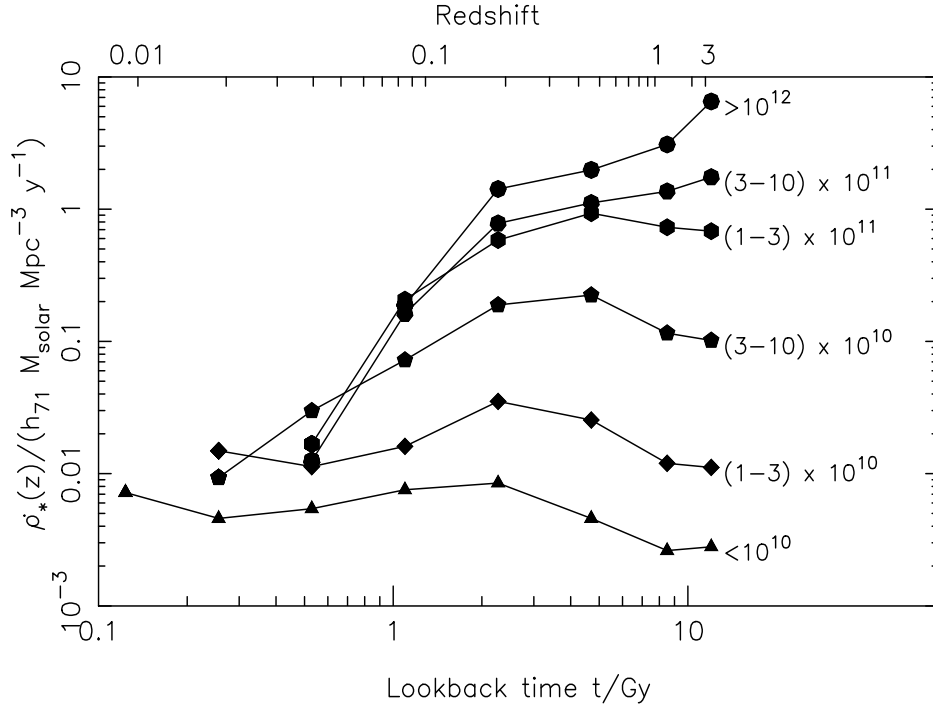


Figure 2: The star formation rate as a function of the observed stellar mass of the galaxy. Labels are in Solar Masses. For clarity, the curves are offset vertically successively by 0.5 in the log, except for the most massive galaxies, which are offset by an additional 1.0. Note the clear trend for galaxies with larger present-day stellar mass to have formed their stars earlier. The bulk of the star formation rate at  $z \simeq 0.5$  comes from galaxies with present-day stellar masses in the range  $3 - 30 \times 10^{10} M_{\odot}$ . Note that the graph makes no statement about when the masses were aggregated. To further test the robustness of our findings we have reconstructed the star formation history changing the dust model and the theoretical stellar populations models. The shape of the star formation history is hardly changed by changing the dust model to the Calzetti extinction law[28], or by using Bruzual-Charlot[29] stellar population models; the latter allows us to assess the effect of systematic errors in our determination of the SFR, since the Jimenez and Bruzual-Charlot models are based on different stellar interior and atmospheres models.

since they are sensitive to the most massive objects only. The fact that we have now discovered that global star-formation activity in fact peaks at rather modest redshift is due to the fact that the peak epoch of star-formation activity in objects of lower (present-day stellar) masses ( $< 3 \times 10^{11} M_{\odot}$ ) was at  $z \lesssim 0.5$ , and that such lower-mass galaxies make a significant contribution to the overall star-formation density. Given present-day observational capabilities, this result could only be revealed by a method such as used here, due to the fact that the fossil record approach allows us to explore the star-formation history of galaxies spanning over two decades in mass. Supplementary information Figure 2 demonstrates consistent results from volume-limited subsamples.

Finally, we note that the mass dependence of peak star-formation epoch revealed in Fig. 2 appears to mirror the mass dependence of black-hole activity as recently seen in redshift surveys of both radio-selected[26] and X-ray selected[27] active galactic nuclei. Such apparently anti-hierarchical behaviour (“downsizing”) is in fact quite consistent with the standard cosmological model, in which galaxies form in small units and merge - our method makes no statement about whether the stellar mass at high redshift was in smaller units or not. The behaviour we see is based on the *present-day* stellar mass of the galaxies, and generally we would expect more massive systems to be part of large-scale overdensities, whose first star formation would occur earlier. Furthermore, these results suggest a very different formation history of low- and high-mass systems, as the mass assembly proceeds in the opposite direction to the star formation. This will be explored in a separate paper.

Correspondence and requests for materials should be sent to Alan Heavens (afh@roe.ac.uk)

**Acknowledgments** We are grateful to Max Pettini, Masami Ouchi and the referees for helpful remarks. The SDSS is managed by the Astrophysical Research Consortium (ARC) for the Participating Institutions. The Participating Institutions are The University of Chicago, Fermilab, the Institute for Advanced Study, the Japan Participation Group, The Johns Hopkins University, Los Alamos National Laboratory, the Max-Planck-Institute for Astronomy (MPIA), the Max-Planck-Institute for Astrophysics (MPA), New Mexico State University, University of Pittsburgh, Princeton University, the United States Naval Observatory and the University of Washington.

## References

- [1] Gallego, J., Zamorano, J., Aragon-Salamanca, A., Rego, M. The Current Star Formation Rate of the Local Universe. *Astrophys. J. Lett.* **455**, 1-4 (1995).
- [2] Lilly, S. J., Le Fevre, O., Hammer, F., Crampton, D.. The Canada-France Redshift Survey: The Luminosity Density and Star Formation History of the Universe to  $z \sim 1$ . *Astrophys. J. Lett.* **460**, 1-4 (1996).
- [3] Steidel, C. C., Giavalisco, M., Pettini, M., Dickinson, M., Adelberger, K. L. Spectroscopic Confirmation of a Population of Normal Star-forming Galaxies at Redshifts  $z > 3$ . *Astrophys. J. Lett.*, **462**, 17-21.

- [4] Connolly, A. J., Szalay, A. S., Dickinson, Mark, Subbarao, M. U., Brunner, R. J. The Evolution of the Global Star Formation History as Measured from the Hubble Deep Field. *Astrophys. J. Lett.* **486**, 11-14 (1997).
- [5] Tresse, L., Maddox, S.J. The  $H\alpha$  Luminosity Function and Star Formation Rate at  $z \sim 0.2$ . *Astrophys. J.* **495**, 691-697 (1998).
- [6] Glazebrook, K., Blake, C., Economou, F., Lilly, S., Colless, M. Measurement of the star formation rate from  $H\alpha$  in field galaxies at  $z = 1$ . *Mon. Not. R. Astron. Soc.*, **306**, 843-856.
- [7] Cowie, L., Songaila, A., Barger, A. J. Evidence for a Gradual Decline in the Universal Rest-Frame Ultraviolet Luminosity Density for  $z < 1$ . *Astron. J.* **117**, 2656-2665 (1999).
- [8] Sullivan, Mark, Treyer, Marie A., Ellis, Richard S., Bridges, Terry J., Milliard, Bruno, Donas, Jos. An ultraviolet-selected galaxy redshift survey - II. The physical nature of star formation in an enlarged sample. *Mon. Not. R. Astron. Soc.* **312**, 442-464 (2000).
- [9] Scott, S., Fox, M., Dunlop, J.S., et al. The SCUBA 8-mJy survey: I - Sub-mm maps, sources and source counts. *Mon. Not. R. Astron. Soc.*, **331**, 817-838 (2002)
- [10] Chapman, S. C., Blain, A. W., Ivison, R. J., Smail, I. R. A median redshift of 2.4 for galaxies bright at submillimetre wavelengths. *Nat* **422**, 695-698 (2003).
- [11] M. Ouchi, K. Shimasaku, S. Okamura, H. Furusawa, N. Kashikawa, K. Ota, M. Doi, M. Hamabe, M. Kimura, Y. Komiyama, M. Miyazaki, S. Miyazaki, F. Nakata, M. Sekiguchi, M. Yagi, N. Yasuda Subaru Deep Survey V. A Census of Lyman Break Galaxies at  $z=4$  and 5 in the Subaru Deep Fields: Photometric Properties. *astroph* 0309657.
- [12] Stanway, E. R., Bunker, A. J., McMahon, R. G. Lyman break galaxies and the star formation rate of the Universe at  $z \sim 6$ . *Mon. Not. R. Astron. Soc.* **342**, 439-445 (2003).
- [13] Shen, S., Mo, H.J., White, S.D.M., Blanton, M.R., Kauffmann, G., Voges, W., Brinkmann J., Csabai, I. The size distribution of galaxies in the Sloan Digital Sky Survey. *Mon. Not. R. Astron. Soc.* **343**, 978-994 (2003).
- [14] Jimenez R., MacDonald, J., Dunlop, J. S., Padoan, P., Peacock, J. A. Synthetic stellar populations: single stellar populations, stellar interior models and primordial protogalaxies *Mon. Not. R. Astron. Soc.*, in press (2003).
- [15] Baldry, I. K. et al. The 2dF Galaxy Redshift Survey: Constraints on Cosmic Star Formation History from the Cosmic Spectrum *Astrophys. J.* **569**, 582-594 (2002).
- [16] Glazebrook, K., Baldry, I. K., Blanton, M. R., Brinkmann, J., Connolly, A., Csabai, I., Fukugita, M., Ivezić, Z., Loveday, J., Meiksin, A., Nichol, R., Peng, E., Schneider, D. P., Subbarao, M., Tremonti, C., York, D. G. The Sloan Digital Sky Survey: The Cosmic Spectrum and Star Formation History. *Astrophys. J.*, **587**, 55-70 (2003).
- [17] Spergel D. N., et al First Year Wilkinson Microwave Anisotropy Probe (WMAP) Observations: Determination of Cosmological Parameters *Astrophys. J. Suppl.* **148**, 175-194 (2003).
- [18] Gordon, K. D., Clayton, G. C., Misselt, K. A., Landolt, A. U., Wolff, M. J. A Quantitative Comparison of the Small Magellanic Cloud, Large Magellanic Cloud, and Milky Way Ultraviolet to Near-Infrared Extinction Curves. *Astrophys. J.* **594**, 279-293 (2003).

- [19] Heavens, A.F., Jimenez, R., Lahav, O. Massive lossless data compression and multiple parameter estimation from galaxy spectra. *Mon. Not. R. Astron. Soc.* **317**, 965-972 (2000).
- [20] Reichardt, C., Jimenez, R., Heavens, A. F. Recovering physical parameters from galaxy spectra using MOPED. *Mon. Not. R. Astron. Soc.* **327**, 849-867 (2001).
- [21] Panter, B., Heavens, A. F., Jimenez, R., Star formation and metallicity history of the SDSS galaxy survey: unlocking the fossil record. *Mon. Not. R. Astron. Soc.*, **343**, 1145-1154 (2003).
- [22] Dickinson, M., Papovich, C., Ferguson, H. C., Budavri, T. The Evolution of the Global Stellar Mass Density at  $0 < z < 3$ . *Astrophys. J.*, **587**, 25-40 (2003).
- [23] Dunlop, J.S. Sub-mm clues to elliptical galaxy formation. In: ‘Deep Millimetre Surveys’, p.11-18, eds. Lowenthal, J.D. & Hughes, D.H., World Scientific (2001)
- [24] Perez-Gonzalez P. G., Gil de Paz, A., Zamorano, J., Gallego, J., Alonso-Herrero, A., Aragon-Salamanca, A., Stellar populations in local star-forming galaxies - II. Recent star formation properties and stellar masses *Mon. Not. R. Astron. Soc.*, 338, 525-543 (2003)
- [25] Fujita S.S. et al, The  $H\alpha$  Luminosity Function and Star Formation Rate at  $z \sim 0.24$  Based on Subaru Deep Imaging Data *Astrophys. J. Lett.*, 586, 115-118 (2003)
- [26] Waddington, I., Dunlop, J.S., Windhorst, R.A., Peacock, J.A. The LBDS Hercules Sample of milliJansky Radio Sources at 1.4 GHz: II. Redshift Distribution and radio luminosity function. *Mon. Not. R. Astron. Soc.*, 328, 882-896 (2001)
- [27] Hasinger, G. The X-ray background and AGNs. In: ‘The restless high energy universe’, Nucl. Physics B. Suppl. Ser., eds. E.P.J. van den Heavel, J.J.M. in ’t Zand, R.A.M.J. Wijers, in press (astro-ph/0310804) (2003)
- [28] Calzetti, D. Reddening and Star Formation in Starburst Galaxies. *Astron. J.*, **113**, 162-184 (1997).
- [29] Bruzual, G., Charlot, S. Spectral evolution of stellar populations using isochrone synthesis. *Astrophys. J.*, **405**, 538-553 (1993).

Supplementary information accompanies the paper on [www.nature.com/nature](http://www.nature.com/nature).